 CMES, vol.3, no.4, pp.447-454, 2002

Simulations of Scuffing Based on a Dynamic System Model

Yuanzhong Hu[1], **Yuchuan Liu, Hui Wang**

Abstract: Scuffing, a major cause of failure in automobile engines, is considered as a dynamic process in this study. Local adhesions may occur randomly in lubricated contacts due to the existence of asperity contact and breakdown of lubricating films. Scuffing would take place if the local events develop rapidly into a large-scale plastic deformation and catastrophic failure. A system dynamic model established in the present paper allows one to predict dynamic behavior of a tribological system through numerical solutions of a group of differential equations. Results show that a transition to adhesion begins when the surface temperature goes beyond a critical value, followed by a rapid growth of the adhesion area. To understand the mechanism of scuffing, further investigations are required.

keyword: scuffing, surface temperature, dynamic system, catastrophic failure

1 Introduction

The study of scuffing can be traced back to more than fifty years ago (Blok, 1937), and great efforts have been devoted to this investigation. Experiments have been carried out on various types of equipment, under different operating conditions, and for different materials. Numerous scuffing criteria have been proposed based on experiment data. While the studies accumulated valuable knowledge, the mystery of scuffing remains unsolved, and design engineers have to largely relay on their experiences to prevent the disastrous failure.

A remarkable feature in the study of scuffing is that confusions and controversies have hung over this research area for many years. The occurrence of scuffing has been attributed to different sources such as instability of hydrodynamic films (Johnson et al., 1988) desorption of active chemical species (Spikes and Cameron, 1974), destruction of surface films (Cuotiongco and Chung, 1994), material plastic flow (Hirst and Hollander, 1974), or accumulation of subsurface damages (Ludma, 1984). Proposed criteria for scuffing show a great variety, including the critical surface temperature (Blok, 1937), maximum PV or PVT values, friction power intensity, subsurface stress, plasticity index, or a combination of temperature, stress and material property (Sheireton et al., 1998a and 1998b). In fact, there is little agreement even on what scuffing is or what its appearance is (Sheireton et al., 1998a). In a well-known definition, scuffing was described as a "localized damage caused by the occurrence of solid-phase welding" (Peterson et al, 1982), but Ludema (1984) believes it should be "a roughening of surfaces by plastic flow".

The confusions have slowed down progresses in scuffing investigation. It is therefore necessary to state a few notions related to this topic.

It is unlikely to expect that scuffing can only start from a single origin. On the contrary, it may initiate from different sources, depending on the operating and lubrication conditions, but ends up with the final failure in a similar form - a large scale welding. Furthermore, scuffing could be excited by random sources, such as a flash temperature or local damages caused by debris.

Scuffing is a process that undergoes successive but different stages. Confusions in the study of scuffing result partly from a misunderstanding that takes a phenomenon in a certain stage of the process as a general feature of scuffing.

The process of scuffing is dynamic in nature. It could either proceed rapidly from a local damage into a large scale welding, or be stopped suddenly at any stage of the course and switch to a running-in process. A remarkable common feature of scuffing is that it goes to a non-linear instability and catastrophic collapse at the final stage of the process.

Based on these considerations, we are trying to develop a theoretical model in this paper to characterize scuffing as a dynamic process. Numerical simulations have been

[1] State Key Laboratory of Tribology, Tsinghua University, Beijing 100084, China

performed on the basis of the dynamic model, and results show that in addition to load and sliding velocity, the environmental temperature plays an important role in the occurrence of scuffing. It has to be emphasized that scuffing is an extremely intricate phenomenon, and what we have done here is only the first step in modeling such a complicated process.

2 A dynamic model of scuffing

The dynamic model established in the present study is for applications in design of piston-cylinder assembly. It is therefore assumed that two lubricated surfaces are in sliding contacts and scuffing may develop in the region of mixed lubrication. The contact geometry of the system is schematically shown in Fig.1.

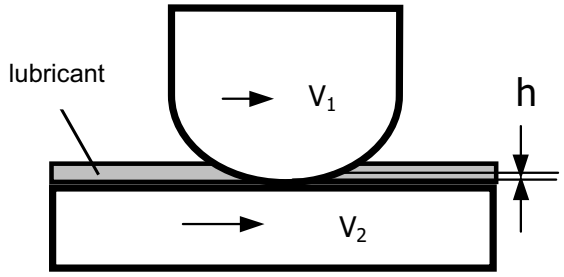

(a)

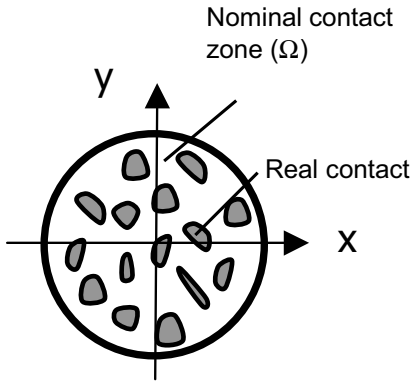

(b)

Figure 1 : Contact geometry and real contact area

The studies on rough surface contact have shown that a nominal contact zone, predicted by the classical theory of elasticity for smooth Hertz contact, is different from the real contact area formed by interacting asperities. In most circumstances, the real contact area takes only a small portion of the nominal zone, as illustrated by an enlarged view in Fig.1(b). Suppose that information on film thickness is available, the real contact area, A_r, for a stationary elastic contact can be estimated by integrating the areas where h is zero.

$$A_{\mathrm{r}} = \int_{\Omega} F(h)\,\mathrm{d}x\mathrm{d}y \tag{1}$$

where Ω denotes the area of the nominal contact zone and F(h) is a topological function defined as

$$F(h) = \begin{cases} 0 & when \quad h > 0 \\ 1 & when \quad h = 0 \end{cases} \tag{2}$$

Asperity contact does not necessarily mean a metal-to-metal adhesion if surface films or absorbed species remain at the contact areas. When these protective surface layers disappear for some reasons, such as high temperature, plastic deformation, etc., a transition from lubricated contact to a microscopic adhesion takes place. Hence, the area of adhesion between two contacting surfaces can be calculated based on equation (2) but with a small modification.

$$A_{\mathrm{w}} = \int_{\Omega} R(T,p,\tau_c)F(h)\,dxdy \tag{3}$$

where A_w defines the area of metal adhesion or so called 'cold welding', and R(T, p,τ_c) is a transition function that describes how many percentages of the real contact area have been converted into direct metal contacts, due to destruction of adsorbed layer or surface films. In general cases, a transition from lubricated contacts to metal adhesion can be caused by several factors, such as the increases in temperature T, normal pressure p, or tangential stress τ_c. In applications to piston-cylinder assemblies where contact pressure is relatively small, it is assumed that the stress-induced transitions are negligible, and temperature becomes the only cause to initiate adhesion. Under this assumption, the transition function R(T, p,τ_c) has the simplest form of

$$R(T) = \begin{cases} 0 & when \quad T < T_c \\ 1 & when \quad T \geq T_c \end{cases} \tag{4}$$

This expression suggests that the transition to metal adhesion occurs at the locations where the local temperature exceeds a critical value, and above the critical temperature, the adhesion area would be independent of T.

Equation (4) contains considerable simplifications of course. First, adhesion may be caused by intense contact pressure. The criterion for the pressure-induced transition relates to the material property, which has not been included in equation (4) due to the assumption of moderate contact condition. Secondly, the adhesion area may keep growing after the transition, or may develop into a large-scale plastic deformation under the combined action of temperature, pressure and subsurface stress. In other words, the value of the transition function could exceed unity, increases continuously, and experiences a second catastrophic change. A full analysis on the nature of the transition function may require an understanding of the material behavior under high temperature and extreme stress, the discussions in this paper are limited to the contact-to-adhesion transition caused by temperature only.

In the present model, scuffing is assumed to initiate from the metal adhesions in microscopic scale. For machine components in contacts under normal operation, the value of A_w used to be small, but the microscopic adhesions may be or may not be developed into scuffing, depending on whether A_w remains stable or grows rapidly. In this sense, the prediction of scuffing becomes a matter of determining the value of A_w and its time evolution.

According to equation (3), the adhesion area A_w depends on four factors: surface temperature T, normal pressure p, film thickness h and tangential stress τ_c. Therefore, the primary task in scuffing prediction is to calculate the distribution and time evolution of the four variables, which can be achieved by solving following equations.

2.1 Surface temperature

Theoretically, the surface temperature Tcan be determined from the equation of heat conduction for solid bodies,

$$\frac{\rho_i C_i}{k_i}\frac{\partial T_i}{\partial t} = \nabla\cdot\nabla T_i \tag{5}$$

with a boundary condition specified as

$$\left.\frac{\partial T_i}{\partial z}\right|_{z=0,h} = \Lambda_i q \pm k_i\,(T_2 - T_1) \quad \text{at the contact surfaces} \tag{6}$$

In equations (5) and (6), the subscript i=1,2 referring to the two surfaces in contact, ρ_i , $C_i$and k_i stand for the density, heat capacity and conductivity of the materials, Λ_i is a coefficient providing the heat partition between two surfaces, and q is the heat generated by interfacial friction, expressed in the form of

$$q = \mu p \mathrm{V} \tag{7}$$

where μ denotes the friction coefficient, p is the normal pressure distribution, and V stands for a sliding velocity.

2.2 Normal pressure

There are two types of pressure coexisting in mixed lubrication, generated by hydrodynamic flow or by asperity contact, respectively. Hence, the normal pressure, p, may be obtained through the Reynolds equation or solid mechanics. In the present study, a new approach presented recently by Hu & Zhu (2000) will be employed, which provides normal pressure distributions over the entire region of mixed lubrication by solving the Reynolds equation and its reduced form.

$$\frac{\partial}{\partial x}\left(\frac{\rho h^3}{12\eta}\frac{\partial p}{\partial x}\right) + \frac{\partial}{\partial y}\left(\frac{\rho h^3}{12\eta}\frac{\partial p}{\partial y}\right) = U\frac{\partial(\rho h)}{\partial x} + \frac{\partial(\rho h)}{\partial t} \qquad (h>0) \tag{8}$$

and

$$U\frac{\partial h}{\partial x} + \frac{\partial h}{\partial t} = 0 \qquad (h \to 0) \tag{9}$$

Questions may arise for the creditability to use equation (9) in the regions of boundary lubrication. However, we believe that as film thickness decreases, the pressure distribution obtained from Reynolds equation will converge to that predicted by the theory of elastic contact, provided the difficulty in numerical solution can be overcome. This notion has been clarified by recent numerical studies, more details can be found in references (Hu and Zhu, 2000).

2.3 Film thickness

Film thickness is given by the following expression.

$$h(x,y,t) = h_0(t) + G(x,y) + \delta(x,y,t) + V(x,y,t) \tag{10}$$

In this expression, $G(x,y)$ is a function describing the geometry of contact bodies, $\delta(x,y)$ denotes the amplitude of composed surface roughness, the third term, $V(x,y,t)$, represents surface deformation caused by the normal pressure, and h_0 relates to the surface distance to be determined through load balance.

$$W = \int_{\Omega} p(x,y)\,dxdy \tag{11}$$

2.4 *Tangential stress*

As discussed previously, a nominal contact zone has to be divided into several parts with different lubrication conditions. As a result, the value of tangential stress, which changes from one region to another, can be described by the following expression.

$$\tau_c = \begin{cases} \mu_f p & \text{for hydrodynamic lubrication} \\ \mu_b p & \text{for boundary lubrication} \\ \mu_a p & \text{for adhesion area} \end{cases} \tag{12}$$

The four variables are strongly coupled with each other, so that equations (5) through (12) have to be solved simultaneously and a numerically.

Equations (3) through (12) present a dynamic model, which provides an opportunity for a numerical simulation of scuffing process if the convergent solutions are available within an acceptable computation time. Unfortunately, the simulation has been limited to the early stage of the process in this paper, due to the difficulty in establishing a mathematical expression for the transition function $R(T,p,\tau_c)$.

3 Determining surface temperature

As stated in the previous section that temperature distributions on contact bodies could be determined through a numerical solution of the equation of heat conduction, but it require a huge amount of computational work, especially when the flash temperatures with sharp spark and very short life are concerned. Since our major interest is the surface temperature, a technique called the 'transient point heat source method' (Carslaw and Jaeger, 1986; Qiu and Cheng, 1998), has been employed in this study to save computation times.

Consider two bodies in a point contact as shown in figure 1, in which the two surfaces move along the x direction with velocities V_1 and V_2. Suppose an instantaneous point heat source of strength $q(x',y',t')dx'dy'dt'$ emitted at position (x',y') and time t' with no heat loss on the boundary. The temperature rises caused by the point heat source was derived by an analytical solution of the equation of heat conduction (Carslaw and Jaeger, 1986). For a distributed heat source, the overall temperature rise at the position (x,y) and time t can be determined consequently, by integrating the elemental temperature rise over the spatial domain Ω and time interval $(0, t)$, which gives an expression in a non-dimensional form of

$$\Delta\overline{T}_i(\overline{x},\overline{y},\overline{t}) = \int_0^{\overline{t}} \iint_{\Omega_c} f_i(\overline{x}',\overline{y}',\overline{t}') \times \frac{\overline{q}(\overline{x}',\overline{y}',\overline{t}')\,d\overline{x}'\,d\overline{y}'\,d\overline{t}'}{(\overline{t}-\overline{t}')^{3/2}}$$
$$\times \exp\left\{ -\frac{[(\overline{x}-\overline{x}') - \overline{V}_i(\overline{t}-\overline{t}')]^2 + (\overline{y}'-\overline{y})^2}{(\overline{t}-\overline{t}')} \right\} \tag{13}$$

In the above equation, the subscript i=1,2 refers to the two surfaces in contact, $f_i(\overline{x}',\overline{y}',\overline{t}')$ denotes the heat partition coefficients that describe how the heat is assigned between two surfaces, and the heat flux density caused by friction can be determined through equation (7) where the friction coefficients μ have different values in different regions, as expressed in equation (12).

The pressure distributions, to be used in calculation of heat flux density q, were obtained with the program developed by Hu & Zhu (2000), which gave the solutions of Reynolds equation (8) and its reduced form (9). The heat flux partition coefficients $f_i(\overline{x}',\overline{y}',\overline{t}')$ were determined by a condition of temperature balance.

Dividing the spatial domain Ω and time period $(0, \overline{t})$ into M×N elements and P time intervals, respectively, equation (13) for the temperature rises may be rewritten into a discrete form.

$$\Delta\overline{T}_i(\overline{x},\overline{y},\overline{t}) = \sum_{k=1}^{P}\sum_{i=0}^{M}\sum_{j=0}^{N} f_i(i,j,k)\overline{q}(i,j,k) \times C_i(i,j,k) \tag{14}$$

where $C_i(i,j,k)$ is the influence coefficient representing the temperature rise at $(\overline{x},\overline{y})$, caused by a continue unit point heat source emitted at (i, j) and in the time interval k.

In order to improve computational efficiency, a moving grid method, used by Ren & Lee (1993) in calculation of elastic deformation, was applied for constructing the influence coefficient matrix for temperature determination. More details on the numerical approach can be found in Liu et al. (2001).

4 Results and discussions

The process of scuffing has been studied numerically by examining the surface temperature, the area of adhesion and their time evolutions. As a preliminary effort in modeling of scuffing, the adhesion triggered by plastic deformation and the final system collapse due to high temperature and stress were not considered. All computations were performed for point contacts, in which an infinite smooth plane slid under a stationary spherical body, whose surface might be either smooth or superposed with a 2D sinusoidal waviness (Fig.1). Different initial body temperatures were applied in order to check their influences on scuffing process. The duration of the process under investigation was 0.236 second, divided into 60 time intervals. As a numerical example to show the capability of the model, values of μ_f, μ_b and μ_a, corresponding to the friction coefficients in the regions of hydrodynamic lubrication, boundary lubrication, and metal adhesion, were chosen from generally accepted database. Other parameters used in calculations are listed in Table 1.

Table 1 : Parameters used in computations

Item	Value
Load W	800 N
Rolling velocity U	100 mm/s
Geometry R_x, R_y	19.05mm
Amplitude of waviness σ	0.4 μm
Wavelength w_x, w_y	$0.5a^2$
Lubricant viscosity η_0	0.096 Pa s
Pressure-viscous coef. αg18.2 GPa^{-1}	18.2 GPa^{-1}
Young's modulus E/	219.78 GPa
Friction coefficient μ_f	0.05
Friction coefficient μ_b	0.1
Friction coefficient μ_a	0.4

4.1 Results for a smooth contact

To verify the model and the numerical approach established in the previous sections, the first numerical example is designed for determining temperature rise in a smooth dry contact, i.e., both surfaces are smooth, no lubricant exists, and the normal pressure obeys a Hertzian distribution. Initially, the lower surface was sliding in a constant velocity. The friction coefficient between the two surfaces is assumed μ_b=0.1. After a period of time (thirty time steps), the sliding was suddenly switched off, and the system relaxed towards the equilibrium. Fig.2(a) gives a temperature distribution on the stationary body, calculated for a given initial temperature T_b=25C$^\circ$ and at the time just before the switch-off of sliding (time step = 30). The shape of temperature distribution looks similar to that of normal pressure, which can be explained by the factor that the pressure dominates the density of heat generation. The maximum surface temperature, which appears near the center of contact circle, has been plotted in Fig.2(b) as a function of time. One can see from the figure that the surface temperature rises in a very short time and then disappears quickly after switching off the sliding. It has to be noticed that the quick response of the system reflects the nature of surface temperature while the body temperature is expected to take much longer time to reach the equilibrium.

4.2 Temperature in mixed lubrication

In this case, an isotropic 2D sinusoidal waviness, with an amplitude of σ=0.4 μm and wavelength of w_x=w_y=0.5a, has been superposed to the surface of the stationary body while the lower smooth plane remains in the same sliding velocity. When lubricant exists, the numerical analysis shows that the two surfaces are in a regime of mixed lubrication with a film ratio of λ=0.13, and a real contact area of 47% (Hu & Zhu, 2000). Fig.3 gives the results obtained at the initial temperature of T_b=25C$^\circ$. Fluctuations in temperature distribution, due to the interacting asperities, are observed in Fig.3(a). However, the general trend of the maximum temperature is similar to the smooth case that the surface temperature rises quickly and reaches a stable value, as shown in Fig.3(b). In this calculation, no transition to adhesion is observed, that is, all asperities are in lubricated contacts. As a result, the maximum temperature is stabilized at a relatively lower level ($T_s \approx$ 120C$^\circ$).

It was found during the computation that the stable value

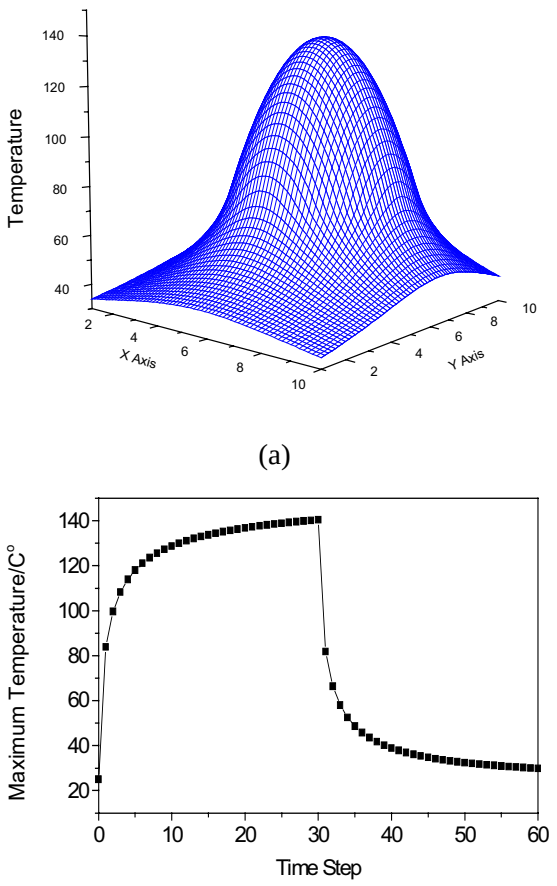

(a)

(b)

Figure 2 : Temperature in a smooth point contact: (a) A 3D view of temperature distribution ($T_b = 25C^\circ$, time step = 30) (b) maximum temperature vs. time

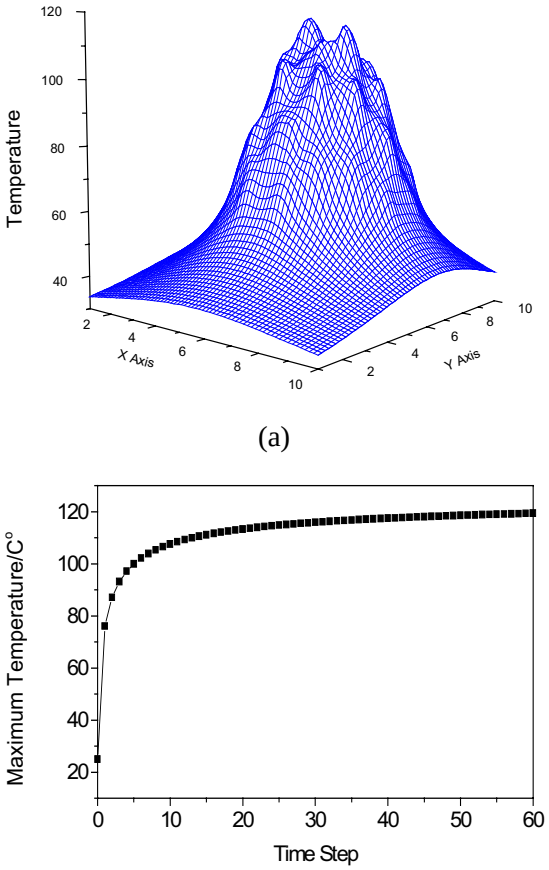

(a)

(b)

Figure 3 : Temperature in mixed lubrication: (a) A 3D view of temperature distribution ($T_b = 25C^\circ$, time step = 60) (b) maximum temperature vs. time

of the maximum temperature depended strongly on the initial temperature T_b. For this reason, we did the same calculation as that presented in Fig.3, but with a higher initial temperature T_b = 110C$^\circ$. In this circumstance, a critical surface temperature T_{cr} for the transition from lubricated contacts to adhesion has to be specified. Unfortunately, the value of T_{cr} would not be available until a series of carefully designed experiment was conducted and the mechanism of the transition was fully understood. To exhibit dynamic behavior of the system, however, a tentative value of T_{cr} = 200C$^\circ$ has been used in the present study. The results in Fig.4(a) show that the temperature distribution is in a similar shape with that in Fig.3(a), but it is stabilized at a higher level. Fig.4(b) gives the maximum temperature as a function of time from which one can see a step jump in T_{max}, indicating that a transition takes place when T_{max} reaches the critical value. The time evolution of the adhesion area, A_w, has been also plotted in the same figure, which demonstrates that the adhesion develops rapidly after the temperature goes beyond the critical value, and all the real contact areas have been transited into adhesion within a very short time. Based on the numerical results, contour plots of the adhesion area at different times have been displayed in Fig.5 that illustrates the development of adhesion.

Fig.4(b) and Fig.5 show the initiation and development of metal-to-metal adhesion. Furthermore, the effect of the initial body temperature can be observed by comparing Fig.4 and Fig.3. For a given combination of materials, contact geometry, surface roughness and operation conditions, there may be a threshold of the initial body temperature, beyond which the adhesion will initiate and

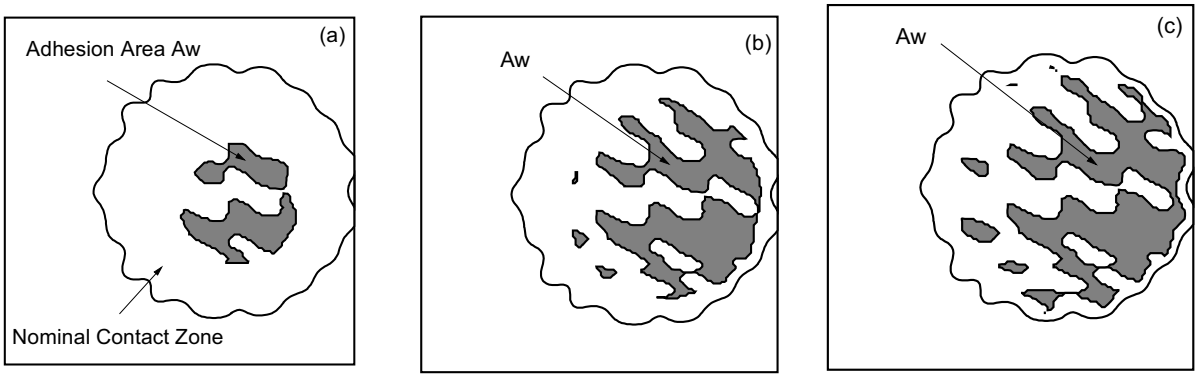

(a) (b) (c)

Figure 5 : Contour plots of adhesion area (a) time step=30 (b) time step=34 (c) time step=60

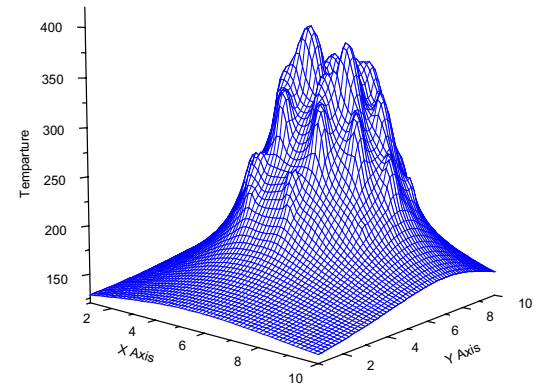

(a)

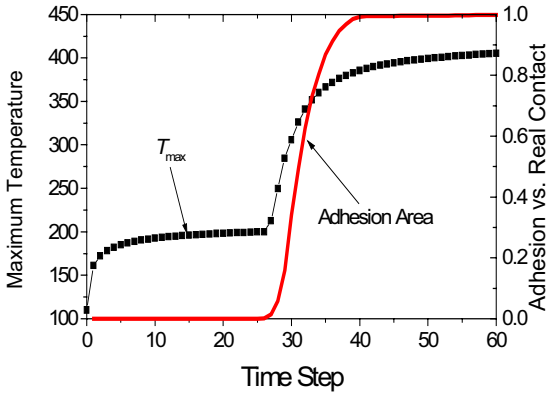

(b)

Figure 4 : Temperature in mixed lubrication: (a) A 3D view of temperature distribution ($T_b = 110C^{\circ}$, time step = 60) (b) maximum temperature vs. time

then grow up quickly.

It is assumed that if surface temperature goes below the critical value, lubrication film will be automatically back in function, healing the adhesion spot. However, this self-healing process was not observed in the above example, partly due to the stationary roughness was employed.

Finally, the numerical results presented in Fig.4 and Fig.5 may not reproduce a complete scuffing process since both temperature and adhesion area were stabilized again after the transition. The adhesion area can be further expanded by a large friction force or shear stress, and the high temperature may soften material, leading to a large-scale plastic deformation under the action of normal pressure and shear stress. Most likely, there will be another transition in the later stage of scuffing, which leads to the final collapse of the system. This will be the next target of the investigation.

5 Conclusions

In the present study, scuffing is considered as a dynamic process that initiates from local or microscopic adhesions and ends up with a large-scale welding. A dynamic system model has been established, which allows to predict dynamic behavior of a tribological system through numerical solutions of a group of differential equations. To improve the computational efficiency, a transient point heat source method has been introduced in evaluation of surface temperature. Results show that a transition to adhesion begins when the surface temperature goes beyond a critical value, and the adhesion area grows rapidly. We realize that scuffing is an extremely complicated phenomenon, and the present work is only a preliminary

effort to develop a numerical model that describes the early stage of the process. To understand the mechanism of scuffing, further investigations in both theoretical and experimental aspects are required.

Acknowledgement: This work was partially supported by the General Motors Corporation under Technology Consortium of GM and Chinese Institutions for Materials and Tribology. We thank Dr. Yucong Wang and Dr. Qihua Liu for their continued support. Invaluable discussions with Dr. Rohit S. Paranjpe, Dr. Fanghui Shi and Dr. Xiaofei Jiang are highly appreciated.

References

Blok, H. (1937): Theoretical study of temperature rise of actual contact under oiliness lubrication conditions, *Proc. General Discussion on Lubrication and Lubricants*, IME, London, Vol. 2, pp. 222-235.

Carslaw, H.; Jaeger, J. (1986): *Conduction of Heat in Solids*, Second Edition, Clarendon Press, Oxford.

Cuotiongco, E. C.; Chung, Y. W. (1994): Prediction of scuffing failure based on competitive kinetics of oxide formation and removal: application to lubricated sliding of AISI 52100 steel on steel. *Tribology Transaction*, vol. 37, pp. 622-628.

Hirst, W.; Hollander A. E. (1974): Surface finish and damage in sliding. *Proc. Roy. Soc.*, Series A, vol. 337, pp. 379-394.

Hu, Yuanzhong; Zhu, D. (2000): A full numerical solution to the mixed lubrication in point contacts. *Journal of Tribology*, vol. 122, pp. 1-9.

Johnson, R. R.; Dow, T. A.; Zhang, Y. Y. (1988): Thermoelastic instability in elliptic contact between two sliding surfaces. *Journal of Tribology*, vol. 110, pp. 80-86.

Liu, Yuchuang; Hu Y. Z.; Wang, W. Z.; Wang, Hui. (2001): Calculation of Temperature distribution of point contact in mixed lubrication (to be published)

Ludema, K. (1984): A review of scuffing and running-in of lubricated surfaces, with asperities and oxides in perspective. *Wear*, vol. 100, pp. 315-331.

Peterson, M. B.; Winer, W. O.; eds. (1982): *Wear Control Handbook, Glossary of terms and definitions in the field of friction, wear and lubrication.* ASME, New York.

Qiu, Liangheng; Cheng, H.S. (1998): Temperature rise simulation of three-dimensional rough surface in mixed lubricated contact, *Journal of Tribology*, vol. 120, pp. 310-318.

Ren, Ning; Lee, S.C. (1993): Contact simulation of three dimensional rough surfaces using moving grid method, *Journal of Tribology*, vol. 115, pp. 597- 601.

Sheiretov, T.; Yoon, H.; Cusano, C. (1998a): Scuffing under dry sliding Conditions – part I: experimental studies. *Tribology Transaction*, vol. 41, pp. 435-446.

Sheiretov, T.; Yoon, H.; Cusano, C. (1998b): Scuffing under dry sliding Conditions – part II: theoretical studies. *Tribology Transaction*, vol. 41, pp. 447-458.

Spikes, H. A.; Cameron, A. (1974): Scuffing as a desorption process – an explanation of the Borsoff effect. *ASLE Trans.*, vol. 17, pp. 92-96.